Astron. Astrophys. 132, 208–218 (1984)

ASTRONOMY AND ASTROPHYSICS

Spectroscopic analysis of extreme metal-poor "dwarfs"

I. Observational material, Fe lines, and model atmospheres*

P. Magain**

Institut d'Astrophysique, Université de Liège, 5, avenue de Cointe, B-4200 Cointe-Ougrée, Belgium

Received June 10, accepted November 3, 1983

Summary. Fe lines are analysed in the spectra of the two extreme metal-poor stars HD 19445 and HD 140283 on the basis of new observational material. It is shown that the use of accurate equivalent widths and very accurate oscillator strengths improves significantly the quality of the analysis. In particular, these stars are found to be more metal-deficient than precedingly thought. This result may imply a significant revision of the adopted abundance scale. It is shown that differential analyses of such stars relative to the Sun are subject to important systematic errors due to the very large difference between the stellar and solar equivalent widths. Finally, the temperature criteria are analysed and it is argued that the criteria linked to deep atmospheric layers, such as the $B-V$ colour or the hydrogen line wings, should not be used to select a model representing satisfactorily the line-forming layers.

Key words: abundance analysis – metal-poor stars – Fe lines

I. Introduction

HD 19445 and HD 140283 are two of the best known extremely metal-poor dwarfs. They have been analysed several times by means of high dispersion spectroscopy. The first of these analyses was published as early as 1951 and the last we are aware of appeared in 1979 (see Table 1). Much progress has been done during that period, but even the last analyses are in many ways unsatisfactory, due mainly to the lack of reliable atomic data – mostly oscillator strengths – combined with the extreme weakness of the spectral lines which makes differential analyses relative to the Sun quite uncertain. In fact, it is easily seen that the main advantage of such differential analyses, i.e. the use of the solar spectrum to derive oscillator strengths, is lost because of the fact that all lines of useful strength in the stars are strongly sensitive to damping in the Sun.

On the other hand, the rather poor quality of the available spectral data prevents to make full use of any method, either absolute or differential, and can even mask the drawbacks of those methods. The main aim of this paper is to show how the quality of such spectroscopic analyses can be improved by the use of very accurate oscillator strengths and good spectral data.

* Based on observations carried out at the Haute Provence Observatory, France

** Aspirant du Fonds National Belge de la Recherche Scientifique

Table 1. Previous [Fe/H] determinations

Star	[Fe/H]	Source
HD 19445	−0.77	Chamberlain and Aller (1951)
	−1.75	Aller and Greenstein (1960)
	−1.75	Wallerstein (1962)
	−2.07	Cohen and Strom (1968)
	−1.18	Grabowski (1976)
	−1.82	Peterson (1978)
	−1.9	Spite and Spite (1978)
HD 140283	−1.04	Chamberlain and Aller (1951)
	−2.48	Baschek (1959)
	−2.03	Aller and Greenstein (1960)
	−2.00	Wallerstein (1962)
	−2.35	Cohen and Strom (1968)
	−1.38	Grabowski (1976)
	−2.36	Peterson (1976)
	−2.4	Spite and Spite (1978)
	−2.60	Peterson and Carney (1979)

II. Observations and reductions

The spectrogrammes were obtained by C. Arpigny at the coudé focus of the 1.52 m telescope at the Haute-Provence Observatory (OHP), France. They were taken on baked IIa-O plates, with a reciprocal dispersion of 12.4 Å mm^{-1} and a width around 0.5 mm. Nine good spectra were obtained for HD 19445 and ten for HD 140283. Two calibration plates were generally available for each spectrogramme.

These spectrogrammes were recorded from 4000 Å to 4900 Å with the Grant microphotometer at the Institut d'Astrophysique de Liège. A calibration curve was recorded every 100 Å on each calibration plate. The wavelength and intensity reductions were carried out with the HP 2100 computer at Liège. The different spectra of the same star were finally co-added, giving a formal signal-to-noise ratio of 100–200, with a resolution of approximately 0.25 Å. The equivalent widths were measured by planimeter and by least squares fitting of gaussian profiles, the latter method allowing to take into account the effect of instrumental blends. The final equivalent widths are means of the two measurements.

Each step was carried out with the greatest care in order to eliminate as far as possible any systematic or accidental error. As

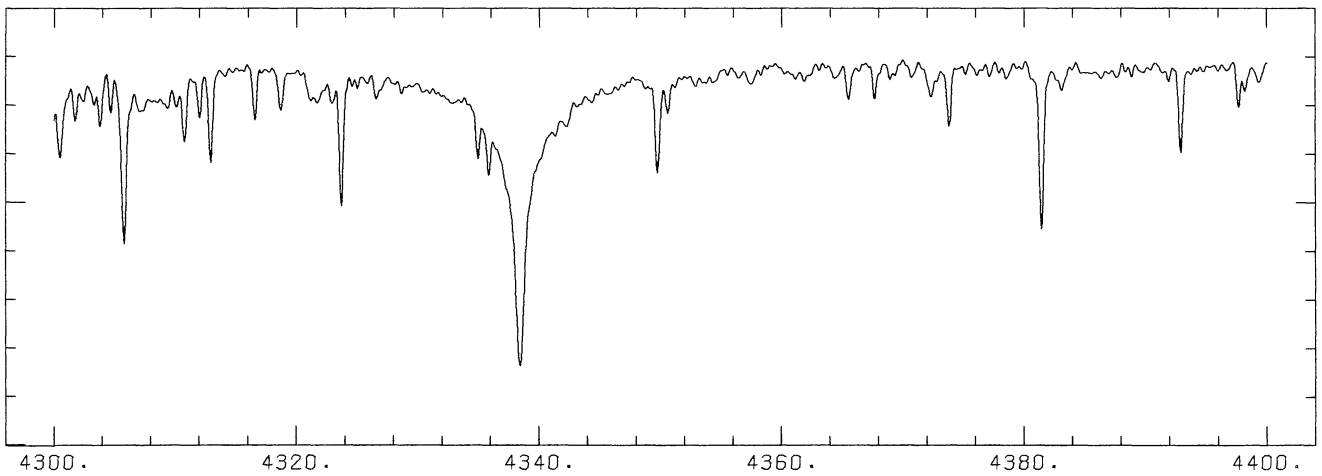

Fig. 1. Spectrum of HD 19445 in the region of H_γ. This spectrum is actually the weighted sum of nine photographic spectra

an example of the quality of the spectra obtained in the way outlined above, we show in Fig. 1 a typical portion of the spectrum of HD 19445.

III. Use of accurate oscillator strengths

We analysed the Fe I lines with excitation potential up to 2.6 eV by using the very accurate oscillator strengths of the Oxford group (Blackwell et al., 1979a, b, 1980a, 1982) which were shown to yield very good results in solar analysis (Simmons and Blackwell, 1982, and references therein).

However, Simmons and Blackwell found a discrepancy between the Fe abundance deduced from a group of lines with excitation potentials around 2.2 eV and all the other groups (with excitation potentials around 0.0, 0.9, 2.3, and 2.5 eV). In fact, the solar abundance deduced from the 2.2 eV lines is systematically 0.077 dex lower than the abundance deduced from the other lines. (A logarithmic abundance scale is used throughout, with $\log N_H = 12$.)

In our stellar analysis, we found a very similar discrepancy, which amounts to 0.073 ± 0.029 in HD 19445 and 0.086 ± 0.036 in HD 140283. The very good agreement of the solar and stellar values might suggest that this discrepancy comes from the atomic data. However, Blackwell (1983, private communication) has checked carefully the oscillator strengths of the lines in question (at least those used in the solar analysis) and concludes that the errors in the published oscillator strengths are of the order of one per cent only. So, there is a genuine abundance anomaly for the 2.2 eV Fe I lines in the solar spectrum at least, and probably in HD 19445 and HD 140283 as well.

As a suggestion for a possible interpretation of the discrepancy, we note that, while the lower and upper levels of the other Fe I lines used in the analyses ionize in low-lying levels of Fe II (a^6D and a^4F), the lower and upper levels of the 2.2 eV lines ionize in rather excited levels (resp. a^4P and a^4D). Moreover, the lower and upper levels of all the 2.2 eV lines analysed so far ionize in *different* Fe II levels. So, any departure from LTE in Fe II might induce an anomaly in the strength of these lines, which would not occur if their lower and upper levels ionized in the same Fe II level (as happens for all the other lines used in the stellar analysis and many of them in the solar case).

In view of the discussion above, we have applied the following correction to the oscillator strengths of the 2.2 eV lines:

$$\log(gf)^{2.2\,\mathrm{eV}}_{\mathrm{used}} = \log(gf)^{2.2\,\mathrm{eV}}_{\mathrm{measured}} - 0.077 \qquad (1)$$

This correction does not mean that the 2.2 eV oscillator strengths are wrong, but is equivalent to group the lines according to their excitation potentials and to analyse each group relative to the Sun. In such a differential analysis, the discrepancy of the 2.2 eV lines, being the same in the Sun and stars, would disappear.

IV. Test of stellar data

a) The very accurate oscillator strengths of the Oxford group can be used to test the internal consistency of the stellar data. Since these gf values are much more accurate than the stellar equivalent widths, the latter are mostly responsible for the dispersion of the abundances computed from different Fe I lines. In Fig. 2, we show the abundances deduced from a set of Fe I lines as a function of microturbulence, for HD 140283. It is seen that the dispersion is lower when our data are used. The same test may be carried with more recent sets of equivalent widths. HD 19445 has been analysed by Peterson (1978) and there are 13 Fe I lines with Oxford gf values in common with our data. So, the comparison is completely straightforward. With the model selected in Sect. VI and a microturbulence of $1.5\,\mathrm{km\,s^{-1}}$, the dispersion of the abundances amounts to 0.05 dex with our equivalent widths and 0.25 dex with Peterson's. The comparison is displayed in Fig. 3, where the abundances computed from the individual lines are plotted versus the line equivalent widths taken from Peterson (1978) and from Table 2. Changing the microturbulence does not significantly alter the comparison. Since for any reasonable choice of microturbulence and stellar model, the dispersion of the results is much lower when our data are used, we may safely conclude that they are of higher quality. The same conclusion would be reached by simply comparing the published dispersions. Our values are between 0.05 and 0.06 dex, while Peterson's are generally in the range 0.15–0.30 dex (see Peterson, 1978, 1980, 1981).

b) For HD 140283, we have at our disposal three higher dispersion photographic spectra, obtained in 1970 at Mount

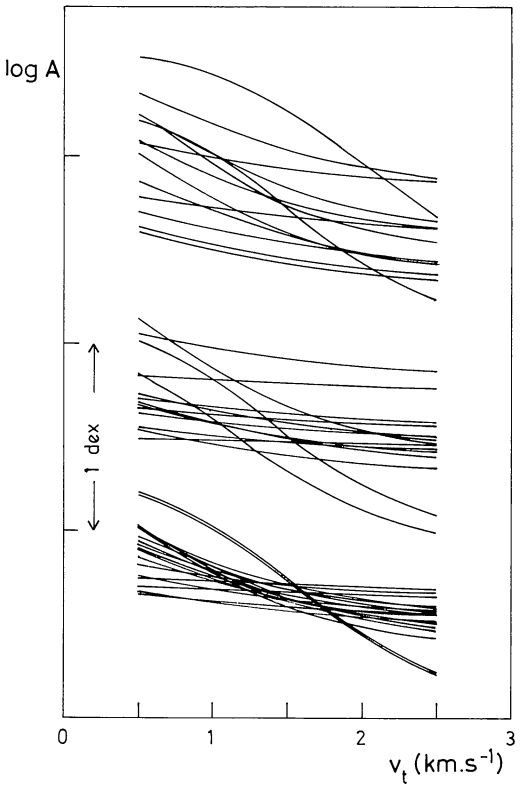

Fig. 2. Variation of line abundance with microturbulence for HD 140283, computed with the 0.93/3.5/−3.0 model. Equivalent widths are from Baschek (1959, *upper part*), Aller and Greenstein (1960, *middle*) and this paper (*lower part*). The different sets are vertically displaced by an arbitrary amount

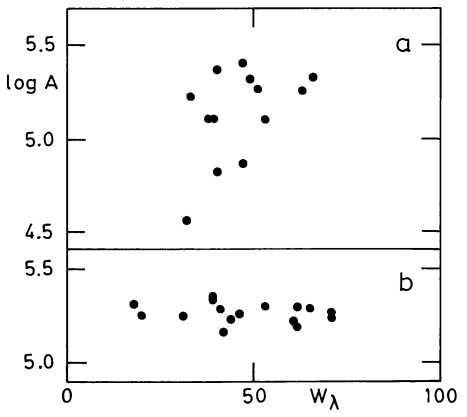

Fig. 3. The abundances deduced from Fe I lines plotted versus line equivalent widths for HD 19445. Equivalent widths are from Peterson (1978, part a) and this paper (part b)

Wilson Observatory by C. Arpigny. Their reciprocal dispersion is 4.4 Å mm^{-1}, corresponding to a resolution around 0.1 Å. These spectra have been reduced in the way outlined above and co-added. In Fig. 4 we compare the equivalent widths measured on these spectra with those from the OHP spectra. No important systematic trend can be detected between the two sets of data. The

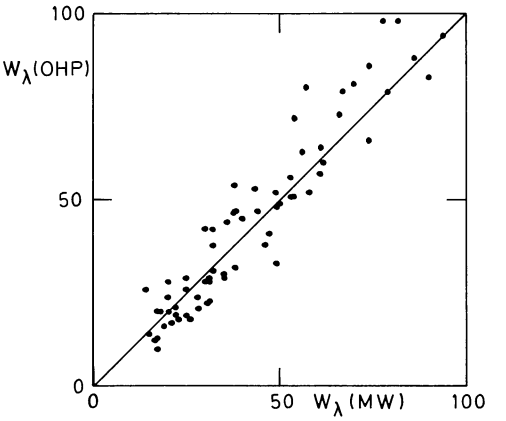

Fig. 4. Comparison of equivalent widths from Haute-Provence (OHP) spectra with those from Mount Wilson (MW) spectra for HD 140283. Equivalent widths are in mÅ. Only lines with $W_\lambda < 100$ mÅ are plotted

r.m.s. dispersion between these two sets amounts to 6.7 mÅ. The analysis of Fe I lines as outlined above indicates that the quality of the OHP equivalent widths is roughly twice better than the quality of Mount Wilson data. (The lower quality of the Mount Wilson equivalent widths might be expected since the number of spectra is smaller and since these spectra are slightly underexposed.) So, the 6.7 mÅ dispersion between the two sets implies a 6 mÅ dispersion in Mount Wilson equivalent widths and a 3 mÅ dispersion in OHP data. The latter is compatible with the 0.05 dex dispersion in computed abundances and with a signal-to-noise ratio better than 100.

c) In summary, our data seem to be free of important systematic errors and are of higher accuracy than previously published data for the stars in question. The last conclusion may seem surprising to the reader since we use photographic plates and since their dispersion is, for example, five times worse than Peterson's Echelle spectra. However, the dispersion does not tell anything about the quality of the data. What matters is: (1) the resolution (2) the signal-to-noise ratio.

Although the dispersion of Peterson's spectra is much larger than ours, the resolution is about the same [0.17 Å in Peterson (1978) to 0.28 Å in Peterson (1980)]. So, the higher quality of our data is mainly due to the higher signal-to-noise ratio, coming from the co-addition of nine or ten good spectra. We should also point out that the large spectral range and the absence of vignetting in the coudé photographic spectra make it much easier to draw the continuum and may contribute significantly to the quality of our data.

V. Method of analysis

The lines used in the analysis are shown in Table 2. They have equivalent widths W_λ between 10 and 100 mÅ. Weaker lines were discarded as having less accurate equivalent widths and stronger ones were rejected to avoid uncertainties due to the poor knowledge of the damping constants. All these lines have oscillator strengths measured by Blackwell and his collaborators, therefore, their excitation potentials lie between 0 and 2.6 eV. The damping

Table 2. Weak Fe I lines

		HD 19445		HD 140283		
λ	χ	W_λ	[Fe/H]	W_λ	$[Fe/H]_1$	$[Fe/H]_2$
4005.25	1.56			86	−2.70	−3.03
4147.67	1.48	39	−2.30	26	−2.56	−3.00
4187.05	2.45	71	−2.30	49	−2.76	−3.06
4187.81	2.42	71	−2.33	51	−2.75	−3.04
4216.19	0.00	42	−2.47	38	−2.63	−3.07
4222.22	2.45	46	−2.40	29	−2.77	−3.07
4233.61	2.48	62	−2.45	47	−2.74	−3.03
4250.13	2.47			56	−2.79	−3.07
4375.94	0.00	61	−2.42	52	−2.68	−3.13
4415.13	1.61			88	−2.69	−3.03
4427.32	0.05	62	−2.33	51	−2.64	−3.09
4430.62	2.22	20	−2.39	13	−2.67	−2.98
4442.35	2.20	41	−2.36	23	−2.80	−3.12
4447.73	2.22	39	−2.29	24	−2.67	−2.98
4461.66	0.09	53	−2.33	45	−2.57	−3.00
4489.75	0.12	18	−2.31	12	−2.60	−3.02
4494.57	2.20	33	−2.43	27	−2.83	−3.15
4528.63	2.18	65	−2.36	46	−2.76	−3.09
4602.95	1.48	31	−2.39	19	−2.75	−3.10

Note: For HD 140283, index 1 corresponds to the model with $\theta_{eff}=0.88$, while index 2 corresponds to $\theta_{eff}=0.93$

constants are computed by the "classical" Unsöld formula (Gray, 1976), with an enhancement factor depending on the excitation potential of the line, as determined by Simmons and Blackwell (1982) from a fit of solar lines. These enhancement factors range from 1 to 6 in C_6 (1 to 2 in $\gamma_6 \div C_6^{0.4}$).

The models used in the analysis are interpolated in a grid of line-blanketed LTE models computed by Gustafsson (1982, private communication) with the same computer programme as the BEGN models (Gustafsson et al., 1975; Bell et al., 1976). Given a stellar model and the atomic parameters of the line, the abundance is computed in LTE by a programme ("ABOND") written by M. Spite at Meudon.

a) Choice of a starting model

The temperature is by far the most critical parameter of the model used in the analysis. We deduced a starting T_{eff} value from the $R-I$ colour index of Johnson's (1966) system. The adopted temperature calibration is that of Peterson and Carney (1979), which is close to Johnson's (1966) one. The $R-I$ observations and the corresponding effective temperatures are collected in Table 3.

The starting metal abundance and surface gravity are much less critical and, so, were chosen after a quick look at the weakest Fe I lines and at the Fe ionization equilibrium.

b) Determination of microturbulence and Fe *abundance*

For each model, the microturbulence is determined in order to suppress the correlation between the deduced abundance and the equivalent widths of the lines. For each line, the abundance is computed for different microturbulent velocities v_t increasing in steps of 0.5 km s^{-1}. For each value of v_t, a straight line is fitted by least squares in the (W_λ, log A) plane:

$$\log A \simeq a(v_t) W_\lambda + b(v_t) . \quad (2)$$

The microturbulence is then interpolated so that $a(v_t)=0$. The formal r.m.s. uncertainty on $a(v_t)$ gives the corresponding uncertainty on the microturbulence, which ranges generally between 0.1 and 0.2 km s^{-1}. Of course, this uncertainty is only internal and does not include any systematic errors, such as those coming from a wrong placement of the continuum. Note that the deduced microturbulence depends only slightly on the chosen damping constants since the stronger lines were selected in order to make a compromise between sensitivity to microturbulence and insensitivity to damping.

We stress that the success of this procedure relies heavily on the quality of the data, mainly oscillator strengths and equivalent widths. For example, the use of previous sets of equivalent widths showed a very poor correlation between abundance and equivalent width for any reasonable choice of the microturbulence (see, e.g., Fig. 2), so that the latter could not be determined with acceptable accuracy.

Table 3. Effective temperature from $R-I$ colours

Star	$R-I$	θ_{eff}	Source
HD 19445	0.33	0.867	Johnson et al. (1968)
	0.35	0.887	Carney and Aaronson (1979)
HD 140283	0.31	0.848	Johnson et al. (1968)
	0.35	0.887	Carney and Aaronson (1979)
	0.36	0.897	Carney (1980)

Once the microturbulence is determined by the method described above, the Fe abundance is obtained as a straight mean of the individual line abundances, at the appropriate v_t. The adopted solar Fe abundance is that deduced by Simmons and Blackwell (1982), corrected for the 2.2 eV discrepancy, i.e. $\log A_{Fe}(\odot)=7.65$. Since this value is obtained by a method very similar to the present one, with the same set of oscillator strengths, the stellar abundance relative to the sun is simply:

$$[Fe/H]=\log A_{Fe}(*)-\log A_{Fe}(\odot). \quad (3)$$

c) Determination of effective temperature

The effective temperature of the star can be determined by requiring the excitation equilibrium to be satisfied: lines of different excitation potentials should give the same abundance. While the accuracy of this procedure relies on the quality of the oscillator strengths and equivalent widths, its reliability is based on the following arguments.

(1) The excitation equilibrium is satisfied in the Sun when the Holweger-Müller (1974, hereafter HM) model is adopted (Simmons and Blackwell, 1982). In other words, if the solar effective temperature was determined via the excitation equilibrium, the right value would be found, as long as the oscillator strengths of the 2.2 eV lines are corrected according to Eq. (1) (see, however, Rutten and Kostik, 1982).

(2) Gustafsson's solar model is fairly close to the HM model in the line-forming region.

(3) If we accept the Fe abundance given by an LTE analysis, we should equally accept the LTE excitation equilibrium, otherwise there is some inconsistency in our procedure.

(4) Strictly speaking, if the excitation equilibrium is not satisfied, the quantity [Fe/H] computed from LTE is not defined since it depends on the excitation potential of the lines used in the analysis.

d) Determination of surface gravity

The standard spectroscopic method for determining the surface gravity of late-type stars is to use ionization equilibria: the ionized lines being much more sensitive to surface gravity than the neutral ones, the gravity is determined by requiring the equality of the abundances deduced from the two stages of ionization.

Unfortunately, the Fe II oscillator strengths are not known with an accuracy comparable to the Fe I ones. Here we use the new arc measurements of Moity (1983), which show good agreement with the solar oscillator strengths of Blackwell et al. (1980b) and, therefore, should be free of important systematic errors. The damping constants used for the Fe II lines are the unmodified Unsöld values. This choice is not critical since all the Fe II lines used in the analysis are rather weak.

In view of the uncertainties present in the determination of surface gravity from the ionization equilibrium, and to check the consistency of the analysis, we also determined the surface gravity by a second method. This method uses the pressure sensitivity of the strong lines situated on the damping part of the curve of growth. We selected a set of five rather strong Fe I lines with oscillator strengths measured at Oxford. All these lines come from levels of excitation potential around 1.5 eV and, therefore, should have nearly the same damping constants. By fitting the profiles computed from the HM solar model – with the appropriate Fe I abundance deduced from the weak lines – to the observed profiles at the centre of the disk (Delbouille et al., 1973), we deduced an enhancement factor of about 1.5 over the Unsöld C_6 value, in good agreement with Simmons and Blackwell (1982). In view of the uncertainties of the procedure (due to uncertainties in the placement of the continuum, weak lines blending the strong line wings, ...), we adopt a rather large error bar and choose as the enhancement factor $\alpha(C_6)=1.5\pm0.5$.

Table 4. Fe II and strong Fe I lines

λ	χ	W_λ(19445)	W_λ(140283)
Fe II			
4178.86	2.58	25	16
4233.17	2.58	49	44
4416.83	2.78	24	13
4508.29	2.85	17	14
4515.34	2.84	22	8
4520.23	2.81	16	12
4555.89	2.83	14	10
4583.84	2.81		36
Fe I			
4045.82	1.48	257	174
4071.75	1.61	155	117
4271.77	1.48	150	105
4383.56	1.48	222	133
4404.76	1.56	171	115

Once the oscillator strengths and damping constants are known, the surface gravity is determined in order that the abundance deduced from the strong Fe I lines agree with the abundance deduced from the weak ones. The main uncertainty of this procedure comes from the poor knowledge of the damping constants. However, it has many advantages over the ionization equilibrium method- most of them coming from the fact that lines of the *same ionization stage* are compared, so that:

– the deduced gravity is independent of the (sometimes rather uncertain) absolute scale of the oscillator strengths;

– it is much less model dependent (e.g., it depends less on the adopted effective temperature);

– it is not directly affected by departures from LTE in the ionization equilibrium.

Furthermore, the fact that these lines are gravity sensitive through the total gas pressure, and not through the electron pressure, is sometimes advantageous.

The Fe II lines and strong Fe I lines used in this analysis are shown in Table 4. Since most of the Fe II lines are rather weak, they are not very sensitive to microturbulence, so that the uncertainty on the deduced abundance comes primarily from the uncertainties in oscillator strengths and equivalent widths. For such weak lines, the relative uncertainty on the equivalent width is proportional to W_λ^{-1} (i.e. the absolute uncertainty is constant). Therefore, the uncertainty of a single abundance determination is roughly proportional to W_λ^{-1} and the Fe II abundance is computed as the mean of the individual values, weighted by the equivalent width of each line.

On the other hand, for the strong Fe I lines, the equivalent width uncertainties come mainly from small blends and should be independent of W_λ. Since the sensitivity of the deduced abundance to the gravity is roughly proportional to $W_\lambda^{1/2}$, the error on an individual $\log g$ determination goes as $W_\lambda^{1/2}$. Consequently, the gravity should be best determined if the abundance deduced from

the strong lines is a mean of the individual values, weighted by $W_\lambda^{1/2}$.

VI. Analysis of HD 19445

From the $R-I$ observations collected in Table 3, we chose $\theta_{\rm eff}=0.87$ as a starting value. For each of the lines gathered in Tables 2 and 4, we computed the abundance with the two following models (notation: $\theta_{\rm eff}/\log g/$[Fe/H]):

(1) 0.87/4.0/−2.3

(2) 0.87/4.5/−2.3

and for three values of the microturbulence: $v_t=1.0$, 1.5, and 2.0 km s^{-1}. The microturbulence, Fe abundance and excitation equilibrium obtained with these two models are shown in Table 5. $\delta\theta_{\rm exc}$ is found from the linear least squares fit:

$$\log A \simeq c-\delta\theta_{\rm exc}\chi\,. \qquad (4)$$

χ being the excitation potential of the lower level and $\theta=5040/T$.

The errors quoted in Table 5 are the r.m.s. uncertainties on the slope for v_t and $\delta\theta_{\rm exc}$, and the standard deviation of the mean for [Fe/H].

The abundances deduced from the Fe II and strong Fe I lines are shown in Table 6. They were computed for each model at the appropriate value of the microturbulence, as determined from the weak Fe I lines. Here again, the quoted uncertainty is the standard deviation of the mean. In Fig. 5 are plotted the abundances computed from the three groups of lines, as a function of the model surface gravity. The error bars take into account:

(a) the standard deviation of the mean,

(b) the error coming from the uncertainty on the microturbulence,

(c) the uncertainty on the damping constant for the strong lines.

It is seen that:

(1) despite the rather large uncertainty on the damping constant, the strong Fe I lines are at least as good as the ionization equilibrium for determining the surface gravity;

(2) the three criteria define an intersection area around $\log g=4.25$ and [Fe/H] = −2.35.

With these model parameters, the excitation equilibrium is very well satisfied (Fig. 6a): $\delta\theta_{\rm exc}=-0.002\pm0.014$. Within the error bars, the excitation equilibrium gives the same effective temperature as the $R-I$ colour: the discrepancy found by Peterson (1978) between these two temperature criteria has been completely removed by the use of accurate equivalent widths and oscillator strengths. Note finally that the uncertainty on $T_{\rm eff}$ coming from the least squares fit of the $\log A(\chi_{\rm exc})$ points amounts to ±90 K, which is of the same order of magnitude as the $T_{\rm eff}$ uncertainties of other methods, such as $R-I$ or $V-K$ colours or hydrogen line profiles. A more detailed discussion of these effective temperature criteria will be given below.

Table 5. Analysis of weak Fe I lines in HD 19445

$\log g$	v_t	[Fe/H]	$\delta\theta_{\rm exc}$
4.0	1.72±0.14	−2.385±0.014	−0.012±0.014
4.5	1.40±0.19	−2.343±0.014	+0.009±0.014

Table 6. Abundances from Fe II and strong Fe I lines in HD 19445

$\log g$	[Fe/H] (strong Fe I)	[Fe/H] (Fe II)
4.0	−2.196±0.041	−2.430±0.065
4.5	−2.421±0.033	−2.211±0.064

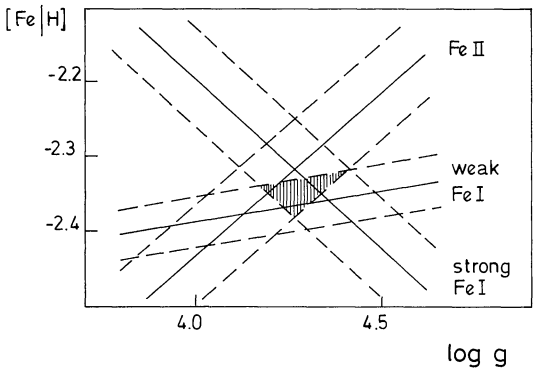

Fig. 5. Determination of surface gravity for HD 19445, with $\theta_{\rm eff}=0.87$

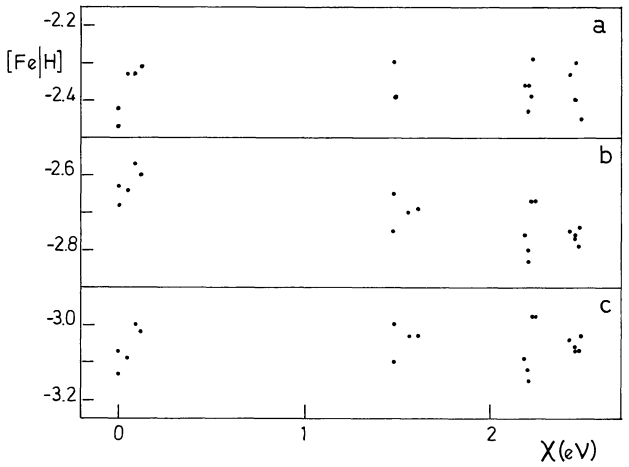

Fig. 6a–c. Excitation equilibria for "absolute" analyses. **a** HD 19445, $\theta_{\rm eff}=0.87$ **b** HD 140283, $\theta_{\rm eff}=0.88$ **c** HD 140283, $\theta_{\rm eff}=0.93$

The following parameters are finally obtained for HD 19445:

$T_{\rm eff}\simeq 5780$ K

$\log g\simeq 4.25$

[Fe/H] ≃ −2.36

$v_t\simeq 1.5$ km s^{-1}.

VII. Analysis of HD 140283

As can be seen from Table 3, the situation is somewhat more confused for this star. Not only the $R-I$ colours show a large scatter, but the same is true for other colour indices such as $U-B$ or $V-R$, and there is also some discrepancy between different

Table 7. Analysis of weak Fe I lines in HD 140283

log$g$	v_t	[Fe/H]	$\delta\theta_{exc}$
3.0	1.66 ± 0.07	-3.078 ± 0.012	-0.005 ± 0.012
3.5	1.51 ± 0.08	-3.029 ± 0.011	$+0.000\pm0.011$

Table 8. Abundances from Fe II and strong Fe I lines in HD 140283

log$g$	[Fe/H] (strong Fe I)	[Fe/H] (Fe II)
3.0	-2.923 ± 0.086	-3.071 ± 0.036
3.5	-3.023 ± 0.066	-2.859 ± 0.036

spectrophotometric scans. This situation makes the determination of effective temperature by means of photometry somewhat unreliable.

The abundances were computed with the starting model 0.88/3.5/−2.7. The results were the following: $v_t=1.67\pm0.13\,\mathrm{km\,s^{-1}}$, $[\mathrm{Fe/H}]=-2.733\pm0.016$, $\delta\theta_{exc}=+0.053\pm0.011$. So, it appears that the temperature is overestimated by some 300 K in the line-forming region (Fig. 6b). Note that a similar problem was encountered by Cohen and Strom (1968) who did not find any model representing satisfactorily the atmosphere of HD 140283 and, finally, carried out the analysis with two different models.

Since we decided to determine the temperature of the line-forming layers by the excitation equilibrium, we recomputed the abundances with the following models:

(1) 0.93/3.0/−3.0

(2) 0.93/3.5/−3.0.

The results of the weak Fe I lines analysis are shown in Table 7, and the abundances computed from the Fe II and strong Fe I lines are gathered in Table 8. As an illustation of the microturbulence determination, we show in Fig. 2 the abundances computed from the individual lines plotted versus the microturbulence for different sets of equivalent widths. With our data, a well defined "neck" is seen around $v_t=1.6\,\mathrm{km\,s^{-1}}$.

The ionization equilibrium points towards a lower surface gravity (log$g\sim3.0$) than the strong Fe I lines (log$g\sim3.5$). However, these "strong" lines, which are actually the strongest Fe I lines in the spectral region considered, are not strong enough in HD 140283 to be good gravity indicators. Indeed, they are more sensitive to microturbulence than to damping. Therefore, the 0.5 dex discrepancy is hardly significant. The extension of the analysis to the near UV spectral region, where some stronger Fe I lines are present, will help to clarify the situation. At the present stage, we propose the following parameters for HD 140283:

$T_{\mathrm{eff}}\simeq5420$ K

log$g\simeq3.2$

$[\mathrm{Fe/H}]\simeq-3.06$

$v_t\simeq1.6\,\mathrm{km\,s^{-1}}$.

VIII. Systematic errors in differential analyses

The two stars analysed here are found to be much more deficient than was generally thought on the basis of previous (mainly differential) analyses. Typical recent values are $[\mathrm{Fe/H}]\sim-1.9$ for HD 19445 and −2.4 for HD 140283. In this section, we compare the present analysis with differential ones to determine the reason of the discrepancy.

The typical differential analysis is the following. For each selected line, the stellar abundance is deduced from the adopted stellar model and measured equivalent width. The corresponding solar abundance is computed for the same line from the solar equivalent width and model. The comparison of the two values gives [Fe/H] for each line. The main advantage of that procedure is that it does not require the knowledge of the oscillator strengths, the latter being deduced from the solar analysis. However, in the case of very weak-lined stars, all the useful lines, although weak in the stars, are strong enough in the Sun to be affected by damping. The solar equivalent widths depend not only on the oscillator strengths, but also on the damping constants, which are not generally well known. If a wrong damping constant is used, a wrong oscillator strength is deduced and the stellar analysis may be affected by important systematic errors, increasing with the overall stellar metallicity (for a given effective temperature).

To illustrate these features, HD 19445 has been analysed by different methods.

Method A
"Absolute" analysis

The Oxford oscillator strengths are used for the Sun and star, both being analysed by using weak lines. Therefore, the lines used are different in the Sun and star and [Fe/H] is obtained by comparing the abundances found in the two cases. This method rests on the hypothesis that the oscillator strengths are free of systematic errors depending on the line strength. This is the method used in this paper.

Method B
"Differential" analysis

For each line, the abundance is computed in the sun and star. The Unsöld value of the damping constant C_6 is used.

Method C

Same as method B with a damping constant C_6 equal to 10 times the Unsöld value (a value typical of past analyses).

Method D

Same as method B with a damping constant equal to $5\,10^{-32}$, the same for all lines. This method mimics the differential analysis with a single curve of growth.

For each of these analyses, we use the same model parameters $\theta_{\mathrm{eff}}=0.87$, log$g=4.0$, $[\mathrm{Fe/H}]=-2.3$ and $v_t=1.5\,\mathrm{km\,s^{-1}}$. For the Sun, we use the HM model with $v_t=0.9\,\mathrm{km\,s^{-1}}$ at the centre of the solar disk. The solar equivalent widths are taken from the catalogue of Moore et al. (1966). The four analyses use the same set of 16 Fe I lines. The resulting Fe abundances and excitation equilibria are shown in Table 9.

In methods C and D, the Fe deficiency is underestimated by about a factor two, due to the overestimate of the damping constants. In method B, the slight underestimate of C_6 is nearly compensated by the systematic underestimate of the Moore et al.

Table 9. Results of different methods of analysis for HD 19445

Method	[Fe/H]	$\delta\theta_{exc}$
A	-2.36 ± 0.01	-0.01 ± 0.01
B	-2.29 ± 0.10	$+0.07\pm0.06$
C	-2.05 ± 0.11	$+0.06\pm0.05$
D	-2.15 ± 0.10	$+0.13\pm0.05$

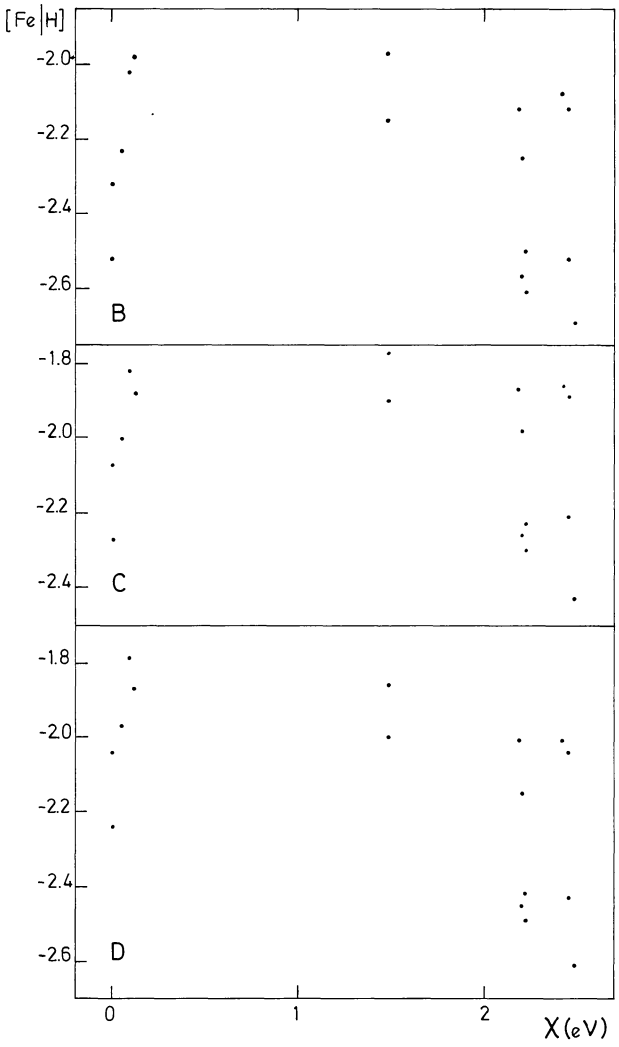

Fig. 7. Excitation equilibria for "differential" analyses of HD 19445. Method as indicated (see text)

equivalent widths. In all differential analyses, the excitation equilibrium is wrong by several hundred Kelvins. This is due to an excitation potential dependent error on the damping constants. This error is more severe in case D since the Unsöld formula represents partly the variation of C_6 with excitation potential.

Finally, note that the use of Moore et al. equivalent widths introduces a bad scatter in the results (Fig. 7). In fact, these equivalent widths are affected by rather large systematic and random errors, which can be partly avoided by using the Liège atlas (Delbouille et al., 1973). However, part of the scatter is due to the fact that many of these lines are badly blended in the solar spectrum, which makes solar equivalent width determinations quite uncertain.

So, we conclude that differential analyses of extreme metal-poor stars relative to the Sun are subject to important systematic errors due to the lack of accurate damping constants. Moreover, if the analysis is carried out in the blue spectral range (which is the spectral region in which most lines are found in the extreme metal-poor stars), the crowding of the lines in the solar spectrum makes many solar equivalent widths very uncertain.

An effect similar to the one found here was noted by Peterson (1980) who found that [Fe/H] values deduced from Oxford oscillator strengths are generally lower than those from solar gf values. However, she attributed the discrepancy to either a wrong choice of the solar Fe abundance or to a wrong choice of the solar and stellar microturbulences. In the present case, these effects are not able to solve the discrepancy since all these quantities are determined rather than chosen arbitrarily. In view of the preceding discussion, it is clear that an important part of the discrepancy is due to the poor knowledge of the damping constants.

IX. Model atmospheres for metal-poor stars

We have seen in Sect. VII that there is some disagreement between the effective temperatures derived from the colours and from the excitation equilibrium for HD 140283. Generally, it is found that different temperature criteria give systematically different effective temperatures when applied to extremely metal-poor stars. The case of HD 19445 is exemplating. For this (pedagogical) star, the temperature criteria can be divided in two classes. The first class criteria give an effective temperature around 5800 K: they are the $R-I$ and $V-K$ colour indices and the excitation equilibrium. The criteria of the second class give an effective temperature around 6050 K: these are the H_β and H_γ profiles and the $B-V$ and Geneva colours properly corrected for blanketing (Magain, 1983). The spectrophotometric scans confirm the discrepancy between the red and blue colours (Fig. 8): if a model is selected so as to match the red-infrared flux, it is seen that it does not reproduce satisfactorily the blue flux: the star is brighter than the model for $\lambda \lesssim 5000$ Å.

As expected, the situation is less clear for HD 140283, mainly due to the poor quality of the colours. However, there is again a discrepancy between the excitation equilibrium, giving an effective temperature around 5400 K, and the hydrogen line profiles, pointing towards an effective temperature close to 5700 K. The spectrophotometry shows the same phenomenon as for HD 19445.

On closer examination, the situation is not as confused as one could think at first sight. In fact, all the temperature criteria which indicate a high effective temperature are sensitive to deep atmospheric layers, while the other ones are related to shallower layers. On the other hand, it is well known that convection (as predicted by the mixing-length "theory") extends to higher layers in the atmospheres of metal-poor stars, as compared with "normal" stars of the same effective temperature and gravity. This can be interpreted in terms of an increased transparency of the atmosphere. Thus, the layers contributing to the bulk of the blue flux and of the hydrogen line wings are much more affected by convection in metal-poor stars than in solar composition stars. A bad treatment of convection (e.g. the mixing-length "theory") should therefore lead to stronger effects in metal-poor stars than in

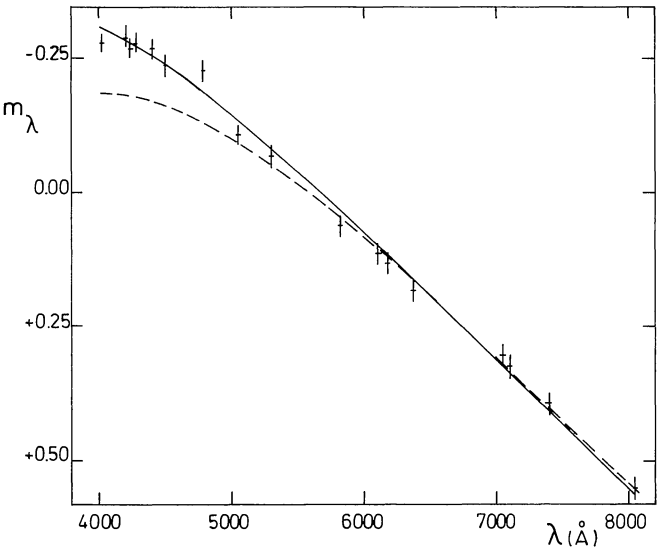

Fig. 8. Continuous flux of HD 19445 (*crosses*) compared with predictions from the theoretical (*dashed line*) and empirical (*full line*) models

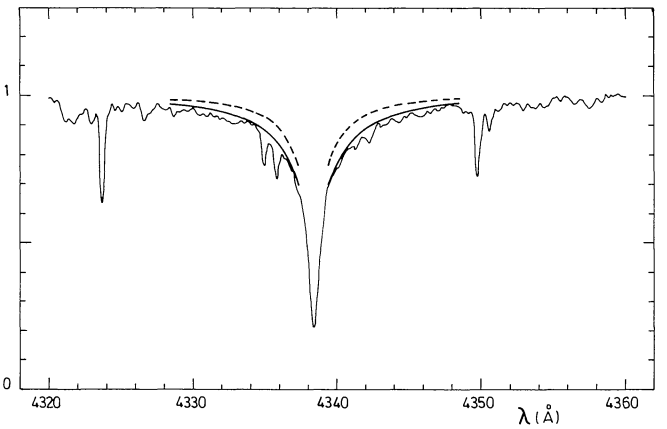

Fig. 9. H_γ profile in HD 19445, along with predictions from the theoretical (*dashed line*) and empirical (*full line*) models

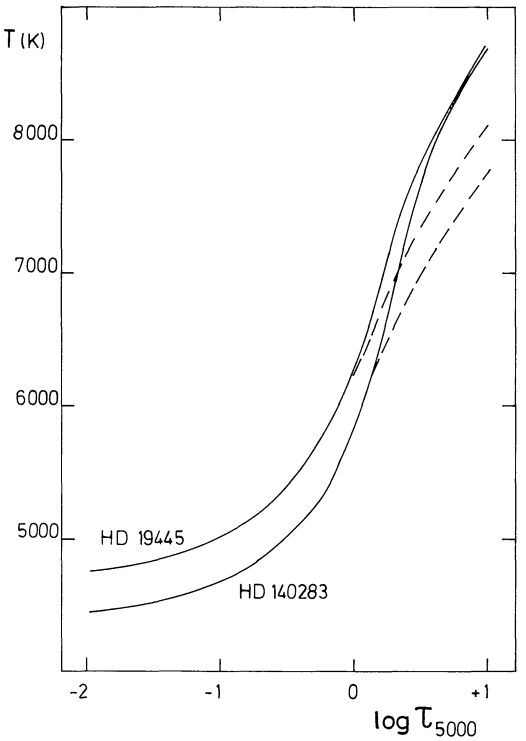

Fig. 10. Temperature structure of the theoretical (*dashed line*) and empirical (*full line*) models

normal ones, and the criteria related to the deeper atmospheric layers should not be used to deduce the effective temperature of metal-poor stars for the purpose of chemical analysis. At the present stage, the best ways to determine the temperature of the line-forming layers seem to be the use of (1) the red-infrared flux and (2) the excitation equilibrium, provided that accurate oscillator strengths and equivalent widths are available over a large range of excitation potential. After all, *lines* should be among the best indicators of the physical state of the *line-forming* layers!

The analysis can then be carried with the model giving the good excitation equilibrium and/or red flux, and one hopes that the wrong treatment of convection does not affect the results too much. Since this procedure is somewhat unsatisfactory, we shall next investigate the effect of changing the structure of these deep layers on the deduced quantities – microturbulence, Fe abundance and surface gravity. The method used is to build an empirical model designed to match the different observations and to carry the whole analysis with this model, exactly in the same way as with the theoretical model. For that purpose, we start from the theoretical $T(\tau)$ relation (τ being the optical depth at 5000 Å) of the Gustafsson's model which gives the good excitation equilibrium and, so, should represent satisfactorily the outer layers. Then, the temperature structure of the deeper layers is changed until the model continuous flux and hydrogen line profiles match the observations. Of course, for a given temperature structure, the other model quantities, such as electron pressure, are computed from the usual set of equations.

The H_β and H_γ profiles were measured on our spectra. The observed continuous fluxes are taken from Christensen (1978), renormalized to the new Vega calibrations of Hayes and Latham (1975) and Tüg et al. (1977). They are corrected for the line absorption by measuring the integrated line equivalent width on our spectra, for each scanner band between 4000 Å and 5000 Å. The correction appears to be fairly small – at most 0.06 magnitude. Of course, windows designed to measure strong absorption features were disregarded. Redwards of 5000 Å, only the continuum windows are taken into account and the line absorption is assumed to be negligible.

The observed continuous flux of HD 19445 is shown in Fig. 8, together with the model fluxes. The H_γ profile is shown in Fig. 9, while in Fig. 10, the theoretical and empirical temperature structures are compared. It is seen that the observations can be matched by changing only the layers deeper than $\tau = 1$, i.e. layers affected by convection. This fact supports the interpretation of a wrong treatment of convection as the cause of the discrepancy. However, we do not argue that the empirical models presented here represent the stellar temperature distributions better than the

Table 10. Comparison of the analyses with theoretical and empirical models

	HD 19445		HD 140283	
	Theor.	Emp.	Theor.	Emp.
v_t	1.57	1.49	1.59	1.50
[Fe/H]	−2.36	−2.42	−3.05	−3.10
log$g$	4.24	4.23	3.25	3.19

Table 11. Sources of error in [Fe/H]

Source	σ(HD 19445)	σ(HD 140283)
W_λ	0.01	0.01
v_t	0.04	0.02
log$g$	0.02	0.05
$T_{\rm eff}$	0.10	0.08
$T(\tau)$ relation	0.06	0.05

theoretical models, nor that they are the unique solution of the observed discrepancy. Other tricks (all related to convection) are equally able to increase the blue flux relative to the red one, e.g. the introduction of temperature inhomogeneities or an increase of the temperature gradient around $\tau_{5000}=1$. The preceding discussion is thus merely intended to show that (1) the reported discrepancies can be removed by simply changing the temperature of the deep layers and (2) the temperature criteria related to these layers should not be used to deduce the temperature of the line-forming layers.

Finally, the two stars are reanalysed with the empirical models. The results are summarized in Table 10. As expected, the changes – being confined to the deeper layers – do not affect much the derived quantities. However, the metal deficiency is slightly increased, due mainly to the increase of the continuous flux in the spectral region considered.

The effective temperatures of the empirical models have been estimated in the following way. If we suppose that the fraction of the flux blocked by the lines is the same in the empirical model as in the theoretical one, the effective temperature of the empirical model $T_{\rm eff}(E)$ is directly related to the effective temperature of the theoretical model $T_{\rm eff}(T)$ by the relation

$$T_{\rm eff}(E)/T_{\rm eff}(T)=[\mathscr{F}_c(E)/\mathscr{F}_c(T)]^{1/4}, \quad (5)$$

where $\mathscr{F}_c$ is the integrated continuous flux of the model considered. Both empirical models appear to be some 100 K hotter than the corresponding theoretical models. If the theoretical models are used, as in Sects. VI and VII, the effective temperature deduced from the excitation equilibrium should not be viewed as the true effective temperature of the star, but more exactly as the effective temperature of the model which represents best the line-forming layers.

X. Conclusion

In Table 11 are summarized the sources of error affecting the final Fe abundance, as determined from the weak Fe I lines, with the estimated contribution of each of these sources to the total uncertainty on [Fe/H]. The following sources of error are considered:

(1) the random errors in the equivalent widths measurements, giving the smallest contribution to the total error in both stars;

(2) the uncertainty on the microturbulence, as determined following the method of Sect. IV;

(3) the uncertainty on surface gravity determined from the ionization equilibrium and strong Fe I lines;

(4) the uncertainty on effective temperature deduced from the Fe I excitation equilibrium;

(5) the uncertainty on the $T(\tau)$ relation in the deeper layers.

The sum of these errors amounts to ~0.2 dex, which is therefore an estimate of the largest possible error on [Fe/H]. Of course, some systematic errors are not taken into account, e.g. possible departures from LTE, effect of temperature inhomogeneities or systematic errors in equivalent widths measurements. For both stars, the dominant source of error in Table 11 is the uncertainty on effective temperature. Two direct improvements of the $T_{\rm eff}$ determination from the excitation equilibrium are possible. First, one could use better equivalent widths to reduce the dispersion of the points in the (χ, A) plane. This is not easy since these stars are rather faint (their visual magnitudes are 8.1 and 7.2) and considerable effort has already been made to obtain accurate equivalent widths. A second – and more promising – possibility is to measure accurate oscillator strengths for lines of higher excitation potential. Again, this is probably difficult, but eagerly needed.

A major uncertainty affecting the analyses of extremely metal-poor stars comes from the lack of a good convection theory, including temperature inhomogeneities and non-local effects, such as convective overshoot. Before such a convection theory is available, perhaps the best we can do is to use as many observations as possible to build reliable empirical models. For that purpose, accurate spectrophotometric observations are urgently needed, including in the infrared.

Acknowledgements. An important part of this work was carried out during a stay of the author at Meudon Observatory. We wish to thank particularly M. and F. Spite for their kind hospitality and their very stimulating advice. We also wish to thank C. Arpigny, N. Grevesse, B. Gustafsson, and B. E. J. Pagel for critical comments on an earlier version of the manuscript. Finally, our thanks are due to D. Blackwell for communicating some results in advance of publication.

References

Aller, L.H., Greenstein, J.L.: 1960, *Astrophys. J. Suppl.* **5**, 139
Baschek, B.: 1959, *Z. Astrophys.* **48**, 95
Bell, R.A., Eriksson, K., Gustafsson, B., Nordlund, Å.: 1976, *Astron. Astrophys. Suppl.* **23**, 37
Blackwell, D.E., Ibbetson, P.A., Petford, A.D., Shallis, M.J.: 1979a, *Monthly Notices Roy. Astron. Soc.* **186**, 633
Blackwell, D.E., Petford, A.D., Shallis, M.J.: 1979b, *Monthly Notices Roy. Astron. Soc.* **186**, 657
Blackwell, D.E., Petford, A.D., Shallis, M.J., Simmons, G.J.: 1980a, *Monthly Notices Roy. Astron. Soc.* **191**, 445
Blackwell, D.E., Shallis, M.J., Simmons, G.J.: 1980b, *Astron. Astrophys.* **81**, 340
Blackwell, D.E., Petford, A.D., Shallis, M.J., Simmons, G.J.: 1982, *Monthly Notices Roy. Astron. Soc.* **199**, 43

Carney, B.W., Aaronson, M.: 1979, *Astron. J.* **84**, 867
Carney, B.W.: 1980, *Astron. J.* **85**, 38
Chamberlain, J.W., Aller, L.H.: 1951, *Astrophys. J.* **114**, 52
Christensen, C.G.: 1978, *Astron. J.* **83**, 244
Cohen, J.G., Strom, S.E.: 1968, *Astrophys. J.* **151**, 623
Delbouille, L., Roland, G., Neven, L.: 1973, Photometric Atlas of the Solar Spectrum from 3000 Å to 10,000 Å, Institut d'Astrophysique de l'Université de Liège, Belgium
Grabowski, B.: 1976, *Acta Astron.* **26**, 147
Gray, D.F.: 1976, The Observation and Analysis of Stellar Photospheres, Wiley, New York
Gustafsson, B., Bell, R.A., Eriksson, K., Nordlund, Å.: 1975, *Astron. Astrophys.* **42**, 407
Hayes, D.S., Latham, D.W.: 1975, *Astrophys. J.* **197**, 593
Holweger, H., Müller, E.A.: 1974, *Solar Phys.* **39**, 19
Johnson, H.L.: 1966, *Ann. Rev. Astron. Astrophys.* **4**, 193
Johnson, H.L., MacArthur, J.W., Mitchell, R.I.: 1968, *Astrophys. J.* **152**, 465
Magain, P.: 1983, *Astron. Astrophys.* **122**, 225
Moity, J.: 1983, *Astron. Astrophys. Suppl.* **52**, 37
Moore, C.E., Minnaert, M.G.J., Houtgast, J.: 1966, NBS *Monographs*, No. 61
Peterson, R.C.: 1976, *Astrophys. J.* **206**, 800
Peterson, R.C.: 1978, *Astrophys. J.* **222**, 181
Peterson, R.C.: 1980, *Astrophys. J.* **235**, 491
Peterson, R.C.: 1981, *Astrophys. J. Suppl.* **45**, 421
Peterson, R.C., Carney, B.W.: 1979, *Astrophys. J.* **231**, 762
Rutten, R.J., Kostik, R.I.: 1982, *Astron. Astrophys.* **115**, 104
Simmons, G.J., Blackwell, D.E.: 1982, *Astron. Astrophys.* **112**, 209
Spite, M., Spite, F.: 1978, *Astron. Astrophys.* **67**, 23
Tüg, H., White, N.M., Lockwood, G.W.: 1977, *Astron. Astrophys.* **61**, 679
Wallerstein, G.: 1962, *Astrophys. J. Suppl.* **6**, 407